JOURNAL OF GEOPHYSICAL RESEARCH, VOL. 113, E00A10, doi:10.1029/2007JE003015, 2008

Temperature, pressure, and wind instrumentation in the Phoenix meteorological package

Peter A. Taylor,[1] David C. Catling,[2] Mike Daly,[3] Cameron S. Dickinson,[1] Haraldur P. Gunnlaugsson,[4] Ari-Matti Harri,[5] and Carlos F. Lange[6]

Received 2 October 2007; revised 3 March 2008; accepted 22 May 2008; published 26 July 2008.

[1] The meteorological package (MET) on the Phoenix Lander is designed to provide information on the daily and seasonal variations in Mars near-polar weather during Martian late spring and summer. The present paper provides some background on the temperature, pressure, and wind instrumentation on the Phoenix MET station and their characterization. A separate paper addresses the MET lidar instrument. Laboratory studies in a Mars wind tunnel confirm estimates that the time constant of the thermocouples should be less than 0.5 s for wind speeds of 5 m s^{-1} or greater. Solar radiation falling on the thermocouples could raise the reported temperatures by up to 0.7 K for wind speeds of 5 m s^{-1}. The increase will be wind speed dependent and will increase to 0.8 K at $U = 3$ m s^{-1} under peak solar radiation. Pressure sensors will give Mars surface pressures accurate to 10 Pa or better while Telltale deflections should provide reliable wind speed information up to at least 10 m s^{-1}. The paper also discusses, to a limited extent, how the MET instruments will be used in conjunction with other instruments on the Phoenix Lander to provide an enhanced meteorological data set. We also describe instrumentation related to the Atmospheric Structure Experiment during entry, descent, and landing (EDL). These instruments will provide deceleration data. Together with drag coefficient information and a surface pressure measurement from MET, these data will allow us to infer the density, pressure, and temperature structure throughout the vertical column during EDL.

Citation: Taylor, P. A., D. C. Catling, M. Daly, C. S. Dickinson, H. P. Gunnlaugsson, A.-M. Harri, and C. F. Lange (2008), Temperature, pressure, and wind instrumentation in the Phoenix meteorological package, *J. Geophys. Res.*, *113*, E00A10, doi:10.1029/2007JE003015.

1. Introduction

[2] In situ measurements of near-surface temperature, pressure, humidity, and wind are essential to improve our understanding of Mars weather and current climate. Phoenix, as the first mission to the high northern latitudes, will provide in situ meteorological information from an environment with a seasonal maximum of atmospheric water vapor [*Tamppari et al.*, 2007] and an expectation of access to subsurface ice. Basic meteorology measurements will support all aspects of the surface science mission and have been included as measurements critical to mission success.

[3] The Phoenix Scout mission was designed with strict cost limits and, in addition, there are significant mass budget constraints. Both have played a role in limiting the amount of meteorological instrumentation that can be carried in the MET package on the Phoenix Lander, but creative use of other instruments (Thermal and Evolved Gas Analyzer (TEGA), Thermal and Electrical Conductivity Probe (TECP), Surface Stereo Imager (SSI), and Robotic Arm Camera (RAC)), along with the MET instrumentation, will allow a more complete set of atmospheric data to be obtained.

[4] Consideration of expected surface conditions as previously observed from orbit and from atmospheric models led to pressure and temperature science requirements being established in the early phase of mission design by the Atmospheric Science Theme Group (ASTG). These included the following:

[5] 1. The payload shall be capable of measuring near-surface temperature at three height levels over at least 0.8 vertical meters continuously at a frequency of 0.5 Hz, in the range 140–280 K, with an absolute accuracy of ±1 K and a resolution of 0.5 K. The uncertainty in the calculated difference between any two concurrent thermocouple readings shall not exceed 0.3 K.

[1] Centre for Research in Earth and Space Science, York University, Toronto, Ontario, Canada.
[2] Department of Earth Sciences, University of Bristol, Bristol, UK.
[3] MacDonald Dettwiler Associates Corporation, Brampton, Ontario, Canada.
[4] Department of Physics and Astronomy, University of Aarhus, Aarhus, Denmark.
[5] Finnish Meteorological Institute, Helsinki, Finland.
[6] Department of Mechanical Engineering, University of Alberta, Edmonton, Alberta, Canada.

0148-0227/08/2007JE003015$09.00

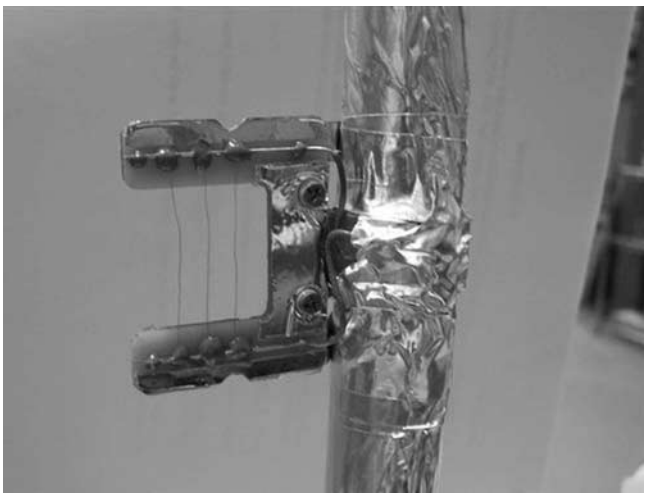

Figure 1. Phoenix MET thermocouples and C Frame.

[6] 2. Phoenix shall be capable of measuring surface barometric pressure at a frequency of 0.5 Hz over a range of 7–11 hPa with (design goal) 10 Pa accuracy and 0.1 Pa resolution.

[7] We had initially hoped to also include an anemometer (hot film or sonic) and a humidity sensor to provide continuous measurements of wind and humidity. These were descoped at a relatively early stage because of a mix of mass, cost, and space qualification issues, but it soon became clear that some wind and humidity measurement was essential in order to assist with the overall goals of the mission. TEGA and TECP can provide some humidity data while the TECP needles have now been tested and calibrated for use as a form of "hot wire" anemometer for wind speed measurement. For wind, however, we wanted an additional sensor capable of determining wind direction and additional, more frequent, speed measurements. Given an engineering constraint that no additional electronic signals were to be permitted at that relatively late stage in the lander development, in addition to severe mass budget constraints, the decision was made to add a small Telltale to the top of the mast. This will be imaged by SSI camera and used to provide an estimate of wind speed and direction at the top of the 1 m MET mast. The corresponding science requirement was that the payload shall be capable of measuring surface winds in two orthogonal directions normal to gravity in the range 2–5 m s^{-1} with an accuracy of 1 m s^{-1} or 20%, whichever is greater and in the range 5–10 m s^{-1} with 40% accuracy. In fact, the Telltale deflection will be interpreted as the direction and speed from which we can compute the two components.

2. Instruments

2.1. Temperature Measurements

[8] Air temperatures and temperature differences between levels will be monitored, almost continuously, by three temperature sensors based on fine wire, butt-welded thermocouples (75 μm diameter, Constantan-Chromel) mounted in C frames on a 1 m mast, coupled with a reference platinum resistance thermometer (PRT) in an isothermal block containing the "cold" junctions of the thermocouples. Levels on the mast are 0.25, 0.5, and 1.0 m above the lander deck, which itself is ~1 m above the ground. There will be three thermocouple junctions in parallel in each of the air temperature sensors, providing a degree of redundancy. Sample thermocouples are shown in Figure 1.

[9] Fine wire thermocouples were selected in part because of a desire for fast response and a modest effect from solar radiation, since no radiation shielding is being used, and in part because of space heritage based on their successful utilization on Viking [*Chamberlain et al.*, 1976; *Larsen et al.*, 2002]. Initially, we had hoped to include three-dimensional turbulent velocity measurements in order to measure fluxes via eddy correlation. As noted in section 1 this has not been possible, but fast response will still be valuable in order to determine turbulent temperature fluctuations, σ_T, and to detect the rapid temperature fluctuations that may be associated with features such as dust devils or sharp frontal passages. A more robust thermistor with a slower time constant may have been an alternative; but heritage is an important factor, and on Viking this type of thermocouple performed very well.

[10] The microvoltages generated by the thermocouple units are measured at 2-s intervals and converted to digital signals with a 16-bit analog to digital converter. Drifts in the readout electronics are calibrated and corrected for at the same time. A total of 256 data records (8.53 min) are buffered and can either be stored at full resolution in the flash memory of MET or processed to provide mean, standard deviation, maximum, and minimum values within the 8.53 min block for storage on the MET unit. The unit can switch autonomously to the full resolution mode, for both temperature and pressure data, on the basis of the magnitude of temperature or pressure fluctuations within the 8.53 min block. The MET unit has its own memory, but data must be transferred to the main lander memory prior to transfer back to Earth via one of the Mars orbiters.

2.2. Pressure Measurements

[11] A Finnish Meteorological Institute (FMI) sensor, based on a silicon diaphragm sensor head manufactured by Vaisala Inc., combined with MacDonald Dettwiler Associates (MDA) data processing electronics will measure pressure. The FMI unit has three pressure sensor heads. One of these is the primary sensor head, and the other two will be used for monitoring the condition of the primary sensor head during the mission. During the mission, the primary sensor will be read with a sampling interval of 2 s and the other two will be read less frequently as a check of instrument health.

[12] The pressure sensor system has a sophisticated real-time data processing and calibration algorithm that allows the removal of temperature-dependent calibration effects. In the same manner as the temperature sensor, a total of 256 data records (8.53 min) are buffered and can either be stored at full resolution or processed to provide mean, standard deviation, maximum, and minimum values for storage on the MET unit.

[13] The time constant of the pressure sensor had not been specified in the formal requirements, but it was originally hoped that it would be short compared to the sampling interval of 2 s. In fact, it is a little longer than that, ~3 s, because of locational constraints and dust-filtering requirements. However, the temporal resolution should still be

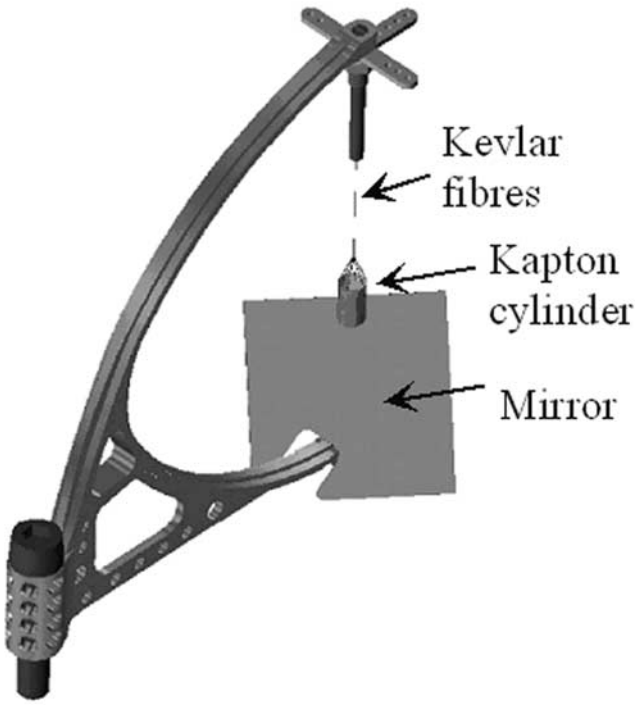

Figure 2. Diagram of the Phoenix MET Telltale.

good enough to detect pressure drops associated with the passage of a nearby dust devil.

2.3. Telltale Wind Measurements

[14] Measuring wind on the surface of Mars is important to understanding passing weather systems and water transport issues. It will also be important in assessing the potential for local dust transport and erosion. Wind information will also aid in choosing the best time of day for sample delivery from the scoop of the robotic arm into Microscopy, Electrochemistry and Conductivity Analyzer (MECA) and TEGA; loss of fine dust blown away by the wind from the sample during this process could affect the validity of the analysis.

[15] As noted in section 1 we had hoped to include an anemometer in the MET package. Faced with a lack of resources to achieve this and with a real desire to have some wind information we decided to make use of the SSI camera and have designed a novel Telltale to achieve this. The Telltale assembly (Figure 2) is made from several parts. The active (deflecting) part of the Telltale consists of a hollow tube of 8 μm Kapton foil deposited with 2 nm Au before assembly. The Kevlar fibers are bonded to the mounting screw and to the Kapton tube. Attached to the mounting screw is an orientation marker, which is a cross-shaped, sandblasted aluminum piece with holes that will serve as a background for mirror images to help determine Telltale deflection and orientation. The mounting screw is attached to the gallows, which in turn is attached to the top of the MET mast. The gallows frame also holds a mirror directly below the Telltale and is inclined in such a way as to allow the SSI camera in its deployed position to see a vertical image of the reflected Telltale.

[16] Small wind velocities will deflect the Telltale in the wind direction with a deflection proportional to the magnitude of the horizontal velocity. At higher velocities the Telltale tends to oscillate because of oscillations in the flow field. The resonance frequency of the Telltale is at about 3 Hz on Mars, and turbulence in this frequency range will be observed as smearing of images. At winds >10 m s^{-1} on Mars the Telltale will start to reach its maximum deflection, laying horizontally, losing its wind speed/deflection correlation ability. Wind directions should, however, still be determined.

2.4. Atmospheric Structure Experiment

[17] In addition to the MET experiment on Phoenix, the atmospheric structure on the day of landing will be derived from measurements of the deceleration of the spacecraft during atmospheric entry. Deceleration is caused by frictional drag that depends on the atmospheric density, pressure, and temperature along the flight path. Previous data sets collected during atmospheric entry were from Viking 1, Viking 2, Mars Pathfinder, and the Mars Exploration Rovers. Phoenix will provide the first in situ atmospheric structure in the high-latitude atmosphere. Vertical atmospheric temperature will provide us with a basis for estimating the saturated vapor holding capacity of the atmospheric column. By examining the temperature profile and comparing with general circulation model (GCM) predictions, it will also help verify radiative calculations and understand net poleward heat transport. The degree of stability of the atmospheric profile bears upon whether convection is likely to be important in transporting dust, water vapor, or other tracers aloft. Mars GCMs predict quiescent large-scale winds in the northern polar region during the northern summer [*Haberle et al.*, 1993]. However, the strong meridional temperature gradient between bare ground and the polar cap generates cyclonic systems [*Hunt and James*, 1979]. The extent to which such weather systems affect atmospheric profiles is unknown. Consequently, a polar atmospheric profile will allow us to better understand the heat budget, dust and water cycles, and dynamical meteorology of the polar environment.

[18] The effects of aerodynamic drag during Phoenix entry are monitored by two inertial measurement units (IMUs) that are located beneath the lander deck on opposite sides of the spacecraft. Each IMU uses three accelerometers for linear acceleration measurement in three Cartesian axes and three ring-laser gyroscopes to measure the three-dimensional angular orientation of the entry vehicle. The IMUs are quasi-commercial products manufactured by Honeywell (Clearwater, Florida,) with part number YG9666BC. The IMUs were selected and configured as part of the active engineering sensing system needed for the critical entry, descent, and landing (EDL) phase of the mission. Consequently, the IMU operational characteristics were wholly driven by EDL engineering demands; use of the IMU data for atmospheric structure reconstruction was a secondary consideration.

[19] Each IMU is internally configured so that it outputs three-axis accumulated linear velocity changes (the time integral of acceleration or ''delta-v'') and three-axis accumulated angle changes (the time integral of angular rate). Unlike previous Mars lander missions, data will be saved onboard at the maximum device output rate of 200 Hz. The IMUs were delivered with a factory calibration based upon

Figure 3a. The calibration tunnel mounted on the door of the Mars chamber. The test section (top, middle) shown here is the one used for solar heating effects.

individual unit testing after assembly. Outputs of delta-v from accelerometers and angle change from gyros are internally compensated for with biases, scale factors, and alignments on the basis of coefficients determined by manufacturer calibration tests. The accelerometers have two stages of digitization that result in pulses and then counts. The final raw digital output is in delta-v units, where one output count is equivalent to 0.0753 mm s^{-1}. However, the final output moves up and down in pulses, which are leaps of many counts, with each pulse equivalent to 2.7 mm s^{-1}. Thus, the amplitude of one pulse is equivalent to 2.7/0.0753 = 35.86 counts, on average. Added to this is noise typically on the order of one count, so that jumps in the raw output are typically 36 or 37 counts. This determines the digital resolution of the raw 200 Hz velocity data to be a delta-v of 2.7 mm s^{-1} and typical noise level to 0.0753 mm s^{-1}. Individual gyros measure the angular rotation in one axis up to a full-scale rate of 375° s^{-1} with a digitization of 0.01144° s^{-1}. Three-sigma noise on the raw gyro output is estimated at 45 microradians.

[20] The noise in the raw digital data can be lowered by integration over selected time intervals, but this is a trade because time integration reduces the vertical resolution in the atmospheric reconstruction. Another consideration is that the IMUs are located neither at the entry vehicle center of mass nor on the symmetry axis. Consequently, consideration of a center of mass frame is needed to take account of spurious components of acceleration measured away from the center of mass. The temperature structure of the atmosphere along the flight path can be calculated from Phoenix IMU data using a four-step process [see, e.g., *Magalhaes et al.*, 1999; *Withers et al.*, 2003] as follows:

[21] 1. The time history of the spacecraft velocity relative to the atmosphere is calculated as a function of altitude by integrating forward the measured velocity changes using the equations of motion and the initial velocity and path angle at entry as a boundary condition. Also, gyroscope data can be integrated to derive the orientation of the spacecraft along the flight path, provided an orientation boundary condition is available at atmospheric entry.

[22] 2. The local atmospheric density is calculated from acceleration along the flight path from the drag equation applied to the spacecraft. This step must be iterated because drag coefficients depend on atmospheric density.

[23] 3. The vertical pressure profile is calculated from integrating the hydrostatic equation for the atmosphere.

[24] 4. Given the density and pressure profiles, the final step is to calculate atmospheric temperature from the ideal gas law.

3. Calibration and Characterization

3.1. Temperature Sensors

[25] The accuracy with which the thermocouples can measure temperature under ideal conditions is a relatively straightforward issue which was addressed by laboratory testing in thermal baths and/or dry wells. This was undertaken by MDA and polynomial calibration curves for individual thermocouples and reference PRTs have been obtained. The other issue is how well the thermocouples will work in a Mars atmosphere; in particular, what will be their time constant, and how will they respond to solar radiation?

[26] In order to address these issues a Mars wind tunnel facility was developed at the Centre for Research in Earth and Space Science (CRESS) Space Instrumentation Laboratory (CSIL) specifically for testing and characterizing the Phoenix MET temperature sensors. Two small wind tunnels (Figure 3a) have been constructed to fit, side by side, in a cylindrical vacuum chamber that can be cooled to Mars temperatures. One tunnel is run with relatively warm air while the other is colder. A switching device (Figure 3b)

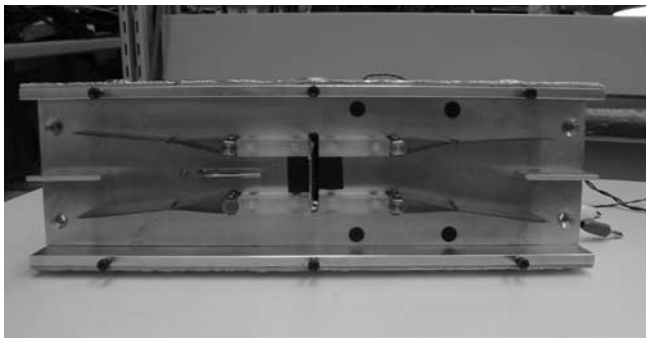

Figure 3b. The switching arrangement for the test section used for time constant studies. Thermocouple C frame is mounted in the central section. The airflow is from right to left and a pitot tube is mounted downstream of the thermocouples to monitor wind speed.

Table 1. Thermocouple Time Constants at a Range of Wind Speeds

Wind Speed ($m\ s^{-1}$)	Time Constant With Decreasing Temperature (s)	Time Constant With Increasing Temperature (s)
4.5	0.504	0.487
6.8	0.465	0.454
16.0	0.349	0.353
19.0	0.318	0.324
24.3	0.291	0.300
27.7	0.282	0.275

allows us to alter the flow through a test section from warm to cold virtually instantaneously, and by monitoring the thermocouple output we can determine the time constant. Once the wind tunnel unit has been installed in the chamber the pressure is reduced to near vacuum (0.6 hPa) and the whole wind tunnel unit is cooled by pumping liquid nitrogen through cooling pipes within it. It is then backfilled with carbon dioxide to Mars pressures, and slight heating is applied to one of the tunnel walls. Tests were conducted in about 8 hPa of CO_2 at temperatures in the range 200–270 K. A range of wind speeds up to 25 $m\ s^{-1}$ was used.

[27] A detailed report on these tests is in preparation, but the essential point is that in these tests the time constant varies from about 0.3 s at 25 $m\ s^{-1}$ to 0.5 s at 4.5 $m\ s^{-1}$ (Table 1 and Figure 4a). In Figure 4b we show the results of analytic and numerical model studies of the time constant together with the experimental results. The experimental determinations generally gave larger time constants than the model studies, which were based on idealized situations.

[28] In addition, we used the same wind tunnel to evaluate the impact of solar radiation on the thermocouples at a range of wind speeds. The thermocouples and their surroundings will both absorb and emit infrared radiation. We are assuming that this will have a small effect, but when solar radiation falls on a thermometer that is not in the shade, the temperature can rise significantly. With a slow response, large heat capacity temperature sensor, e.g., a mercury thermometer or large thermocouple, it is customary to shade the sensor so that it is not exposed to direct sunshine. For very fine wire thermocouples this is not the usual practice, and one relies on more efficient conduction of heat between the air and the thermocouple to reduce the impact of solar heating. In addition, the thermocouples are moderately reflective.

[29] Simulated solar radiation was generated with a xenon lamp and filters and then directed onto the thermocouples in the C frame within the wind tunnel through an optical fiber. By turning the lamp on and off at regular intervals, we were able to detect the temperature increase reported by the thermocouples. This also provided another measure of the time constant. The tests were repeated at a range of wind speeds. Tests were conducted with both clean and dust-coated thermocouples. Sample results for a wind speed of 5.1 $m\ s^{-1}$ are shown in Figure 5, and results for a range of temperatures and a wind speed of about 3 $m\ s^{-1}$ are listed in Table 2. Solar radiation intensities were matched to the maximum expected at the lander site, and tests were run both at Mars and room temperatures. We found that our optical fibers lost transmission capacity at temperatures below −40°C. However, for $-40°C < T < 0°C$ we found minimal variation and very similar solar radiation effects were obtained at room temperature. Radiation effects on the thermocouples varied with wind speed and were less than the 1° accuracy requirement for wind speeds greater than about 1 $m\ s^{-1}$. Even with zero wind speed, thermal

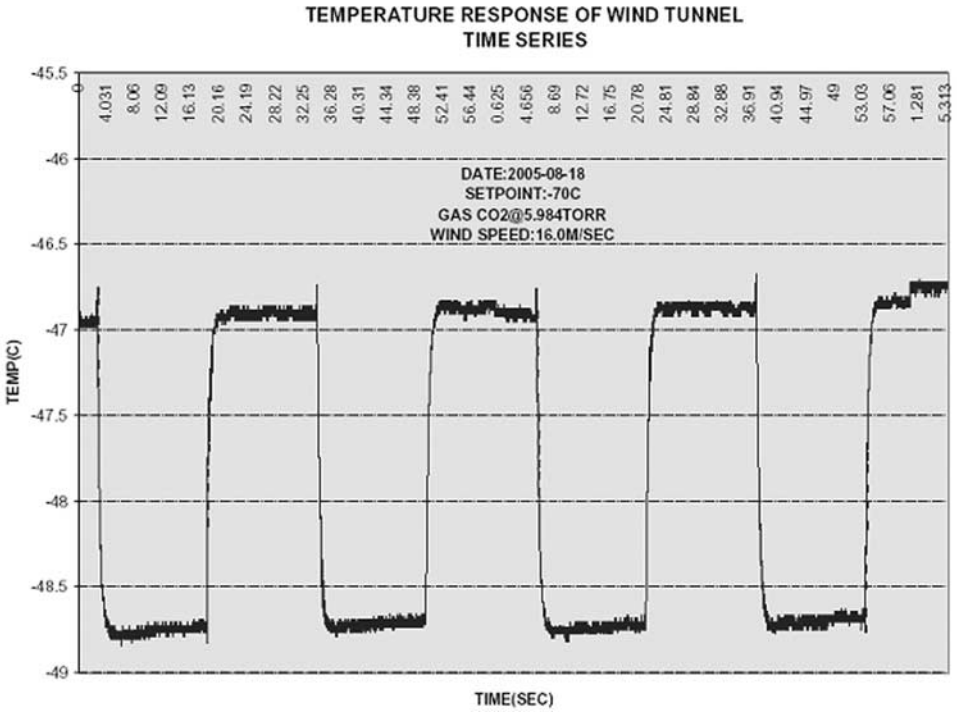

Figure 4a. Sample record for switched flow through four temperature cycles with wind speed 16.0 $m\ s^{-1}$.

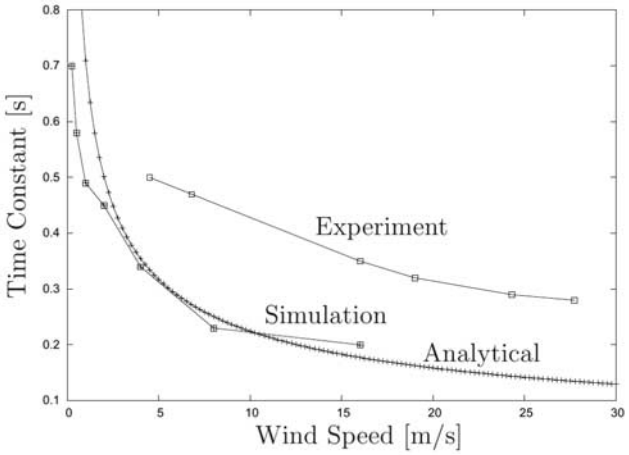

Figure 4b. Analytical and numerical model determinations of thermocouple time constants.

diffusion kept the temperature difference to 1.08°C. For temperature differences between levels it is assumed that both levels will be exposed to the same amount of solar radiation.

[30] An additional issue being researched using both physical and numerical models is the impact of flow distortion and thermal contamination due to the lander itself. Noting that the lander is a fairly bluff body and that the mast is only 1 m above a deck which stands ~1 m above the surface, we must expect that the flow past the temperature sensors will not necessarily have come from the same upstream elevation and that the measurements of temperature may also be affected by thermal diffusion or plumes emanating from the lander. Studies of both of these effects are underway in order to help interpret temperature and temperature profile measurements to be made once the lander has arrived on Mars. Note that on some occasions we will have additional air temperature measurements from the TECP allowing us to extend the height range of the profiles to include near-surface measurements.

Table 2. Temperature Increase Caused by Solar Radiation at Different Temperatures[a]

Test	Reference Temperature (C)	Temperature Difference (C)	Pressure (hPa)	Wind Speed (m s^{-1})
1	−56.1	0.163	7.96	3.10
2	−49.2	0.435	7.96	3.05
3	−42.5	0.668	7.96	3.00
4	−36.4	0.829	7.96	2.90
5	−30.7	0.815	7.96	2.90
6	−25.5	0.813	7.95	2.80
7	−20.7	0.793	7.94	2.70
8	−16.2	0.785	7.94	2.76

[a]Low values at cold temperatures are due to reduced transmission of light by the optical fiber bundle. Xenon lamp + 1 AM0 filter. MDA thermocouple S/N 207 with York thermocouple as reference.

3.2. Pressure Sensor

[31] Calibration of the engineering and flight model pressure sensors were conducted by FMI over a range of pressures and temperatures. These calibration coefficients were used by the readout electronics to calculate pressure. System level tests that included the flight readout and data processing electronics were conducted at MDA and verified the FMI calibration.

[32] To conduct these tests, the Phoenix and reference pressure sensors were inserted in a controlled pressure and temperature enclosure, backfilled with CO_2. Pressure and temperature were varied over appropriate ranges, and the Phoenix sensor output was compared with a calibration standard. There were initial discrepancies associated with the calibrator, but a thorough investigation and subsequent

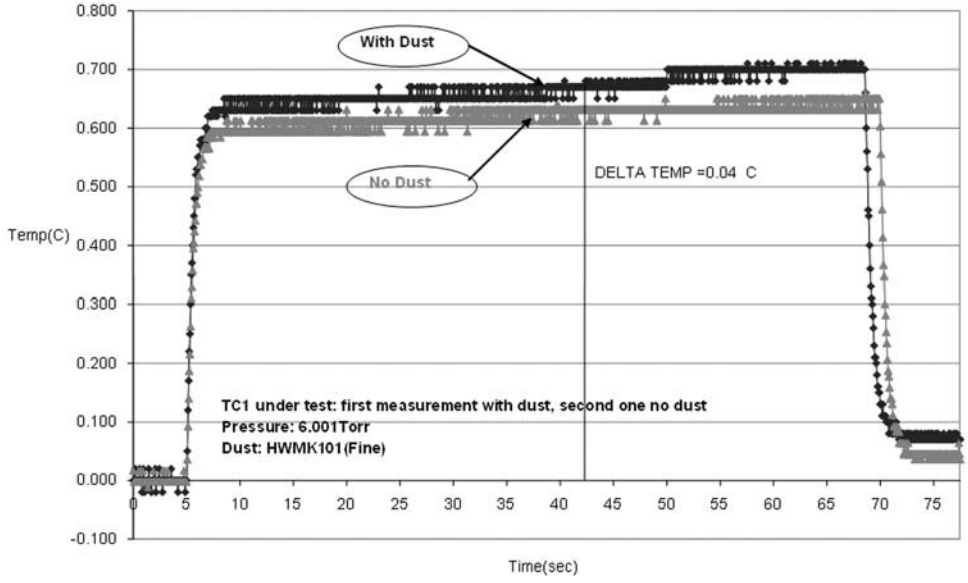

Figure 5. Tests of effect of solar radiation on the thermocouples. Wind speed 5.1 m s^{-1} in CO_2 at 8 hPa. One data set with simulated Mars dust, HWMK 101, deposited on the thermocouples by a dust sprayer. Temperature offsets are shown.

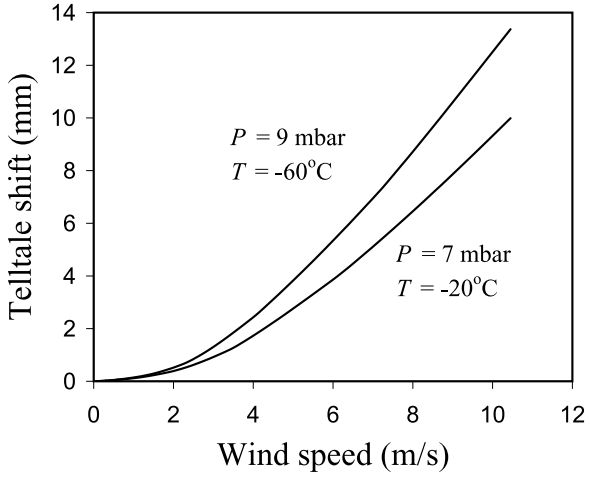

Figure 6. Horizontal shift of the Kapton part of the Telltale calculated under the conditions indicated and wind direction perpendicular to the line of sight from the SSI.

retest satisfactorily confirmed that the sensors could meet project requirements.

3.3. Telltale

[33] Details of the characterization of the Telltale are presented in a separate paper [*Gunnlaugsson et al.*, 2008]. A series of measurements were employed in order to derive all characteristics of the experiment and develop a mathematical model of the performance/deflection as a function of wind speed. This was necessary in order to separate the effect of gravity differences between Earth and Mars on the Telltale for predicting deflection angles as a function of wind speed on Mars. Figure 6 shows deflection as a function of wind speed for two typical conditions on Mars.

4. Discussion

[34] Our first goal with the Phoenix MET station is to collect in situ, surface data for the landing site. While Viking and Pathfinder have made measurements in equatorial and midlatitude locations, these will be the first in situ polar measurements made on Mars. This will allow us to check model predictions and remotely sensed estimates of near-surface air temperatures and pressures and their variation over a diurnal, and part of a seasonal, cycle. We are depending on the Telltale and SSI camera, on the TECP to provide some information on the wind, and on the lidar to give us information on boundary layer height.

[35] Given the diurnal cycle of solar insolation and large day/night variations in near-surface temperature we are predicting a strong diurnal cycle in turbulence and in the near-surface wind speeds, with relative calms at "night," even though the Sun may remain above the horizon. This will be useful practical information for the mission in terms of sample collection and delivery to the TEGA and MECA analysis sites. While the Phoenix Lander site may be quite variable meteorologically because of variations in dust loading and the relative proximity of the polar ice cap [cf. *Tamppari et al.*, 2008] we can note that the Viking and Pathfinder data show relatively stable diurnal temperature cycles [*Tillman et al.*, 1994; *Larsen et al.*, 2002]. Coupled with temperature variance and temperature gradient information from the temperature sensors on the mast, optical depth from the SSI camera, and also from profiles with the TECP temperature sensors on the end of the robotic arm, we will also extract information relative to the surface energy budget.

[36] TEGA humidity and water vapor deuterium to hydrogen (D/H) ratio measurements, together with frost and fog observations with the SSI and RA cameras, will allow us to piece together the movement of water vapor between the air and the surface and subsurface. During the period of the Phoenix mission it is anticipated that water vapor will be ablating from the northern polar ice cap and moving southward. Measurements of wind speed and direction from the Telltale; humidity from TEGA; humidity, temperature, and wind speed from the TECP; and boundary layer depth and dust distribution from the lidar will help to establish boundary layer features and fluxes of moisture and thus improve our understanding of the water cycle of the planet.

[37] In all of these investigations we must recognize that we have only very basic near-surface measurements at a single location. Some data (T and p) will be virtually continuous while other measurements can only be made intermittently when power and other scheduling conflicts permit. In particular, there may be limitations on measurements at night, although we will be able to secure some diurnal cycle information. As a result, models of the Martian boundary layer will play an important role in data assimilation and interpretation as they have for Viking and Pathfinder [*Savijärvi*, 1999]. *Taylor et al.* [2007] present some model results on dust distributions within the boundary layer for 70°N, while other coupled boundary layer and dust modeling and large eddy simulation studies are ongoing. Mars global circulation models [e.g., *Moudden and McConnell*, 2005] and model databases [*Lewis et al.*, 1999] have been used to help in the determination of the meteorological conditions we expect to find at the Phoenix site. Comparisons of these predictions with the observed climate will be a good test of these models.

[38] **Acknowledgments.** The Canadian component of this NASA mission, including the work of the MET science team, has been funded by contracts and grants from the Canadian Space Agency (CSA). MDA was the prime contractor for MET with significant hardware contributions from FMI, JPL, and the Mars Simulation Laboratory at the University of Aarhus. The construction of the Telltale has been supported by the Faculty of Science at the Universities of Aarhus and Copenhagen and grants from the Danish Natural Science Foundation. The leader of the overall project is Peter Smith, University of Arizona, while Allan Carswell, Diane Michelangeli, and James Whiteway have led the MET science team. CSA personnel, Alain Ouellet, Vicky Hipkin, and Marcus Dejmek, have also assisted the science team. Many individuals have worked on the instrumentation and its calibration, but in particular, we should acknowledge the contributions of Stephen Brown, Di Wu, and Konstantin Baibakov at York; Olajide Akinlade and Jeff Davis at University of Alberta; Andrew Kerr at MDA; and Stephane Lapensee, Claude Brunet, and Isabelle Tremblay at CSA.

References

Chamberlain, T. E., H. L. Cole, R. G. Dutton, G. C. Green, and J. E. Tillman (1976), Atmospheric measurements on Mars-The Viking meteorological experiment, *Bull. Am. Meteorol. Soc.*, *57*, 1094–1099, doi:10.1175/1520-0477(1976)057<1094:AMOMTV>2.0.CO;2.

Gunnlaugsson, H. P., et al. (2008), The Telltale wind indicator for the Mars Phoenix Lander, *J. Geophys. Res.*, doi:10.1029/2007JD003008, in press.

Haberle, R. M., J. B. Pollack, J. R. Barnes, R. W. Zurek, C. B. Leovy, J. R. Murphy, H. Lee, and J. Schaeffer (1993), Mars atmospheric dynamics as

simulated by the NASA Ames general circulation model: 1. The zonal-mean circulation, *J. Geophys. Res.*, *98*, 3093–3123, doi:10.1029/92JE02946.

Hunt, G. E., and P. B. James (1979), Martian extratropical cyclones, *Nature*, *278*, 531–532, doi:10.1038/278531a0.

Larsen, S. E., H. E. Jørgensen, L. Landberg, and J. E. Tillman (2002), Aspects of the atmospheric surface layers on Mars and Earth, *Boundary Layer Meteorol.*, *105*, 451–470, doi:10.1023/A:1020338016753.

Lewis, S. R., M. Collins, P. L. Read, F. Forget, F. Hourdin, R. Fournier, C. Hourdin, O. Talagrand, and J.-P. Huot (1999), A climate database for Mars, *J. Geophys. Res.*, *104*, 24,177–24,194, doi:10.1029/1999JE001024.

Magalhaes, J. A., J. T. Schofield, and A. Seiff (1999), Results of the Mars Pathfinder atmospheric structure investigation, *J. Geophys. Res.*, *104*, 8943–8955, doi:10.1029/1998JE900041.

Moudden, Y., and J. C. McConnell (2005), A new model for multiscale modeling of the Martian atmosphere, GM3, *J. Geophys. Res.*, *110*, E04001, doi:10.1029/2004JE002354.

Savijärvi, H. (1999), A model study of the atmospheric boundary layer in the Mars Pathfinder lander condition, *Q.J.R. Meteorol. Soc.*, *125*, 483–493, doi:10.1002/qj.49712555406.

Tamppari, L. K., M. D. Smith, D. S. Bass, and A. S. Hale (2007), Water vapor behavior in the north polar region of Mars as seen by MGS TES, paper presented at 38th Lunar and Planetary Science Conference, Lunar and Planet. Inst., Houston, Tex., 12–16 Mar.

Tamppari, L. K., J. Barnes, E. Bonfiglio, B. A. Cantor, A. J. Friedson, and A. Ghosh (2008), The atmospheric environment expected for the Phoenix landed season and location, *J. Geophys. Res.*, doi:10.1029/2007JE003034, in press.

Taylor, P. A., P. Y. Li, D. V. Michelangeli, J. Pathak, and W. Weng (2007), Modelling dust distributions in the atmospheric boundary layer on Mars, *Boundary Layer Meteorol.*, *125*, 305–328, doi:10.1007/s10546-007-9158-9.

Tillman, J. E., L. Landberg, and S. E. Larsen (1994), The boundary layer of Mars: Fluxes, stability, turbulence spectra and growth of the mixed layer, *J. Atmos. Sci.*, *51*, 1709–1727, doi:10.1175/1520-0469(1994)051<1709:TBLOMF>2.0.CO;2.

Withers, P., M. C. Towner, B. Hathi, and J. C. Zarnecki (2003), Analysis of entry accelerometer data: A case study of Mars Pathfinder, *Planet. Space Sci.*, *51*, 541–561, doi:10.1016/S0032-0633 (03)00077-1.

D. C. Catling, Department of Earth Sciences, University of Bristol, Wills Memorial Building, Bristol BS8 1RJ, UK.

M. Daly, MacDonald Dettwiler Associates Corporation, 9445 Airport Road, Brampton, ON L6S 4J3, Canada.

C. S. Dickinson and P. A. Taylor, Centre for Research in Earth and Space Science, York University, 4700 Keele Street, Toronto, ON M3J 1P3, Canada. (pat@yorku.ca)

H. P. Gunnlaugsson, Department of Physics and Astronomy, University of Aarhus, Ny Munkegade 54, DK-8000, Aarhus C, Denmark.

A.-M. Harri, Finnish Meteorological Institute, Erik Palmenin Aukio 1, FI-00560 Helsinki, Finland.

C. F. Lange, Department of Mechanical Engineering, 4-9 Mechanical Engineering Building, University of Alberta, Edmonton, AB T6G 2G8, Canada.